

High-Sensitivity Raman Spectroscopy of Supercritical Water and Methanol over a Wide Range of Density

Yoshiro Yasaka, Masahito Kubo, Nobuyuki Matubayasi, and Masaru Nakahara*

Institute for Chemical Research, Kyoto University, Uji, Kyoto 611-0011

Received March 19, 2007; E-mail: nakahara@scl.kyoto-u.ac.jp

High-sensitivity Raman vibrational spectroscopic equipment was developed to study the hydrogen-bonding structure in supercritical fluids over a wide density range. Supercritical water was investigated to the very dilute region of 0.1 MPa (3×10^{-4} g cm^{-3}) at 400 °C, and the spectroscopic profile at the isolated state was observed. For comparison, supercritical methanol was also investigated, and the effect of the alkyl group on the hydrogen bonding is elucidated. For both water and methanol, the OH stretching peak shifted toward a lower frequency with an increase in the density as a result of hydrogen-bond formation. The red shift relative to the isolated value was not always proportional to the density. In the case of water at 400 °C, the shift was nonlinear over a wide density range; it was almost linearly dependent on the density between 0.6 and 0.2 g cm^{-3}, whereas at lower densities, the dependence became steeper. For methanol, a nonlinear density dependence was similarly observed at a corresponding reduced temperature. The density dependence then became more linear at higher temperatures. The density dependence of the spectroscopic profile is interpreted in terms of the matrix of force constants affected by the formation of hydrogen bonding.

Supercritical fluids have emerged as a potential medium for chemical and geophysical processes of industrial and environmental importance.[1,2] In particular, supercritical hydrogen-bonding fluids, such as water and methanol, are rich in their solvation and reaction behaviors. The macroscopic phase behavior of one-component supercritical fluid is well-known through a variety of efforts since van der Waals' days,[1,3–14] and the current target is a molecular-level understanding of the solvations and reactions. The spectroscopic methods including both vibrational (IR and Raman) and magnetic resonance (NMR) as well as the diffraction methods, such as X-ray and neutron, have already been applied to supercritical fluids.[1,5–34] With the advance of high-temperature and high-pressure techniques, the spectroscopic methods have successfully shown the microscopic structure of supercritical fluids. In this work, a highly sensitive Raman spectroscopic system was developed and applied for supercritical water, which is the most clean and green fluid but requires the severest experimental control.

We have previously developed an NMR probe for high-temperature and high-pressure regimes in cooperation with JEOL and have investigated the hydrogen-bonding structure and dynamics of supercritical water.[5–7] The NMR spectroscopic method has been proven to be advantageous to extract averaged information on the molecular level, such as the average number of hydrogen bonds, the self-diffusion constant, and the reorientational correlation time; the spectral feature is simple due to the motional narrowing and useful for the statistical–mechanical interpretation. Although NMR spectroscopy is powerful in structural identification of the species due to high spectral resolution (<1 Hz), its resolution along the time axis is relatively low, since the relaxation time is particularly elongated at high temperatures. Here lies the possibility for the vibrational spectroscopies, such as IR and Raman, to provide additional molecular insights when their resolution and sensitivity are high enough. Vibrational spectroscopy is complementary to NMR in the sense that it is likely to probe the structural components of fluid and is rather fast to collect the data.

The purpose of this work was to develop a new high-temperature and high-pressure apparatus for Raman spectroscopy and to study supercritical hydrogen-bonding fluids over a wide range of densities (pressures). Water (H_2O) and methanol (CH_3OH) were measured to a very dilute region approaching the zero-density limit. We chose Raman, instead of IR, since our main concern was aqueous solutions under supercritical conditions; the IR absorption by water itself is too strong for quantitative measurements of such solutions. The density dependence of the Raman peak shift was then characterized in terms of the linearity and compared to previous NMR results.[5,8–11] Especially, since a very low-density regime of supercritical water can now be examined by NMR from both the static and dynamic perspectives,[7] the complementary Raman study is desirable to cover the low-density regime. We show that the correspondence between the Raman shift and the NMR chemical shift is distinct between water and methanol. A matrix of force constants was employed to interpret how the effect of the hydrogen bonding appears differently in the Raman and NMR results.[9–11,23–28]

Recently, supercritical methanol has been studied on the molecular level by spectroscopic and diffraction methods.[9–11,23–28] Due to the methyl group on one end, methanol has only one OH bond and does not have the symmetry that is enjoyed by water. Lack of the symmetry, as well as losing one hydrogen-bonding site, may play an important role in the density dependence of the hydrogen bonding and the corresponding spectroscopic profile. Thus, a close comparison with water over a wide range of densities is important for understanding the nature of the vibrational profile of the hydrogen bonding at supercritical states. One advantage of studying

Published on the web September 13, 2007; doi:10.1246/bcsj.80.1764

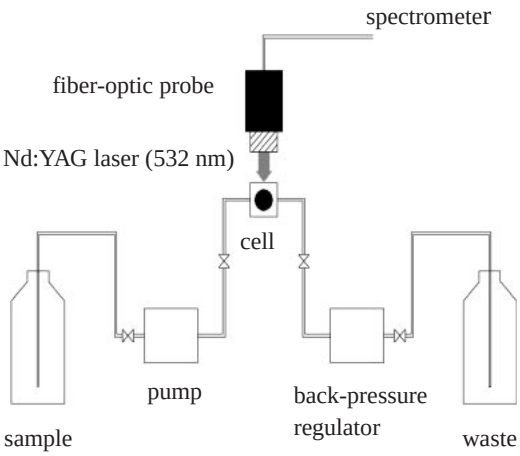

Fig. 1. Schematic diagram of the Raman system.

methanol arises from its lower critical temperature (≈240 °C) and pressure (≈8 MPa). States significantly above the critical point can be achieved much more easily for methanol than for water. By studying a wide range of thermodynamic states for methanol, the temperature dependence of the spectroscopic profile can be elucidated.

Experimental

Apparatus. A schematic diagram of the supercritical Raman system is shown in Fig. 1. A supercritical cell was connected to a pressure-regulating chamber that controls the flow of a liquid or gas sample through stainless pipes attached. The sample flow could be tuned between 10^{-3} to 10 mL min^{-1}. The pressure was raised by an HPLC pump (JASCO PU-2080 Plus) before the sample enters the supercritical cell, and the pressure was controlled by a back-pressure regulator (JASCO SCF-BPG), after the sample passed through the supercritical cell. The pressure was finely tuned between zero and 50 MPa with an interval of 0.1 MPa. The pressure was kept within an error of 0.1 MPa from the target pressure. The supercritical cell was made of Inconel 625. The capacity of the cell was as small as 12 μL to suppress the multiple scattering. The sample flow was kept at 0.1 mL min^{-1} throughout this study. The cell was sealed in a chamber that was kept in vacuum by an air pump for the purpose of thermal insulation and minimization of the spectroscopic noise due to air dust. The sample was heated in the supercritical cell with a ceramic heater. The temperature could be set as high as 450 °C with an interval of 0.1 °C. The temperature was detected by a Chromel-Alumel thermocouple at the cell and regulated by a controller (Chino KP1000).

An overview of the supercritical flow cell is shown in Fig. 2. A 532 nm Nd:YAG Laser (Spectra Physics Millenia IIi) beam was back-scattered, collected and sent to a high-sensitivity spectrometer (Renishaw RM1000B) connected via an optical fiber cable. The Rayleigh line was effectively filtered out, and the photon counting was performed by using a CCD camera. An advantage of collecting back-scattered light, instead of conventional 90 degree scattering, is evident, because the scattering intensity is far greater in the direction parallel to the laser. The resolution of the spectrometer was less than 2 cm^{-1}. The measurements were done with a relatively low laser power of 108 mW. Instead of a sapphire window, we used a diamond window, which was as thin as 0.6 mm and was connected to a metallic pedestal by a special

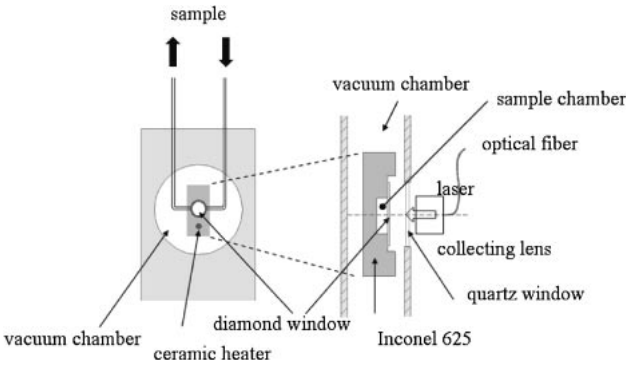

Fig. 2. Schematic diagram of the supercritical flow cell.

technique patented by Sumitomo Electric Industries, Ltd. Since the window was thin enough, the distance between the sample and the collecting lens could be as short as 1 cm. Thus, a wide solid angle of $\approx\pi$ sr is assured so that the back-scattered light is collected by the detector with minimal loss. The diameter of the diamond window was 3.5 mm, whereas that of the collecting lens was 20 mm. In addition, the diamond window gave a sharp peak at 1334 cm^{-1}, which was convenient for the calibration of the spectrometer.

Procedures. Water was purified to a specific conductance of 5.6×10^{-6} S cm^{-1} using the Milli-Q Labo. filter system (Milli-Q Pore). Initially, water was gradually heated at a constant pressure of 40 MPa until 400 °C. This state had a density of 0.52 g cm^{-3}, and corresponded to a reduced temperature (T_r) of 1.04 and a reduced density (ρ_r) of 1.63; $T_c = 647$ K, $\rho_c = 0.32$ g cm^{-3}. The pressure was then gradually decreased to 0.1 MPa. During the isothermal pressure (density) decrease, the measurement time at each wavenumber was 30 s for the pressures between 40 and 20 MPa (0.10 g cm^{-3}). At the lower pressures, the measurement time was increased accordingly so that the totally symmetric OH stretching band signal intensity obtained became roughly equal at each pressure. The measurement time was 120 min at the lowest pressure of 0.1 MPa. The spectra were taken between the wavenumbers of 4500 and 500 cm^{-1}.

For methanol, spectroscopic grade methanol (purity, 99.6%) was purchased from Nakalai Tesque Inc. Measurements were done at temperatures of 250, 300, 340, and 400 °C. These temperatures correspond to the reduced temperatures of $T_r = 1.02$, 1.12, 1.20, and 1.31, respectively, where $T_c = 512.6$ K. The measurement time was set similar to that of water with the shortest time of 30 s at higher pressures. It was 65 min at 0.5 MPa and 400 °C. The spectra were taken between the wavenumbers of 4500 and 500 cm^{-1} for methanol as well.

Results and Discussion

Pressure and Temperature Dependence of Spectral Features. First, we demonstrate the sensitivity of our Raman apparatus. Low-density spectra of pure supercritical water at 0.1 MPa and methanol at 0.5 MPa are shown in Fig. 3. Both were taken at 400 °C. The OH stretching bands for water and methanol were clearly observed at 3657 and 3687 cm^{-1}, respectively, in agreement with the isolated gas values at lower temperatures.[13,15,24,35–37] For water, the totally symmetric mode was observed preferentially by Raman in contrast to IR.

The pressure dependence of the Raman spectrum of water in the stretching region at 400 °C is shown in Fig. 4a. The wave-

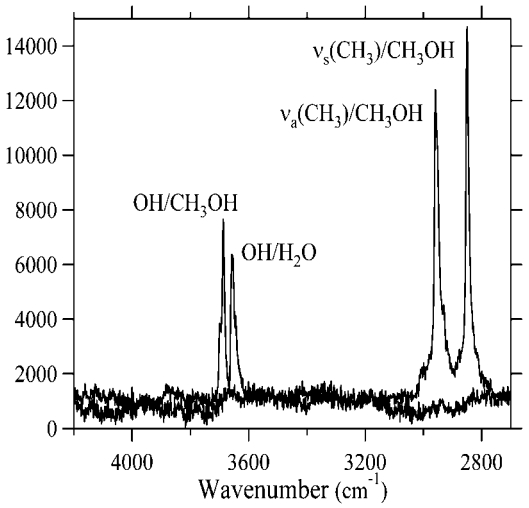

Fig. 3. Raman spectra of H_2O (0.1 MPa) and methanol (0.5 MPa) at 400 °C. The resolution is $\approx 1\,cm^{-1}$. Peaks between 3000 and 2800 cm^{-1} represent the symmetric and anti-symmetric stretching of CH_3 of methanol.

number at the peak position could be clearly identified and is plotted against the density in Fig. 4b. When the density (pressure) was reduced isothermally, the totally symmetric (ν_1) peak shifted toward a larger wavenumber with a fairly constant slope ($\approx 80\,cm^2\,g^{-1}$) until a density of $\approx 0.2\,g\,cm^{-3}$. However, there was a significant change in the density dependence between 0.2 and 0.1 $g\,cm^{-3}$. At 0.1 $g\,cm^{-3}$ and below, the peak shift rate again became fairly constant with a larger rate ($\approx 250\,cm^2\,g^{-1}$). At a density of $\rho = 3.3 \times 10^{-3}\,g\,cm^{-3}$ and pressure of 1.0 MPa, the peak was at 3657 cm^{-1}, which is identical to the monomeric value within the experimental precision.[13,15,35,36] We could obtain spectra down to a density of $3.2 \times 10^{-4}\,g\,cm^{-3}$ (pressure: 0.1 MPa) and found no more changes in the spectral feature.

With respect to the peak positions at high and medium densities, there is good agreement between the present and previous results.[13,15–17] Among the previous studies, Ikushima et al. have investigated down to as low as one third of the critical density at 400 °C.[17] For densities $\geq 0.13\,g\,cm^{-3}$, our results agree with theirs, whereas they do not agree at $0.10\,g\,cm^{-3}$. The integrated signal intensity is also provided in Fig. 4c. It was proportional to the photon count per unit time at the thermodynamic state of interest. Evidently, the intensity increases nonlinearly with the density. When the density is high, the transition to a vibrational excited state occurs cooperatively due to the intermolecular correlations (coupling of the polarizability derivatives), and the signal intensity is enhanced. Thus, the nonlinear increase in the signal intensity with the density is also an indication of intermolecular correlations.

For comparison, the methanol OH stretching peak was investigated at 250, 300, 340, and 400 °C ($T_r = 1.02$, 1.12, 1.20, and 1.31, respectively). Recently, supercritical methanol has been studied by NMR chemical shift and spin–lattice relaxation, Raman, X-ray, and neutron diffractions, ultraviolet/visible and IR spectroscopies, and molecular dynamics simulation.[9–11,23–28,38–41] Due to its lower sensitivity compared to IR,[9–11,23–28] the application of Raman spectroscopy was limited

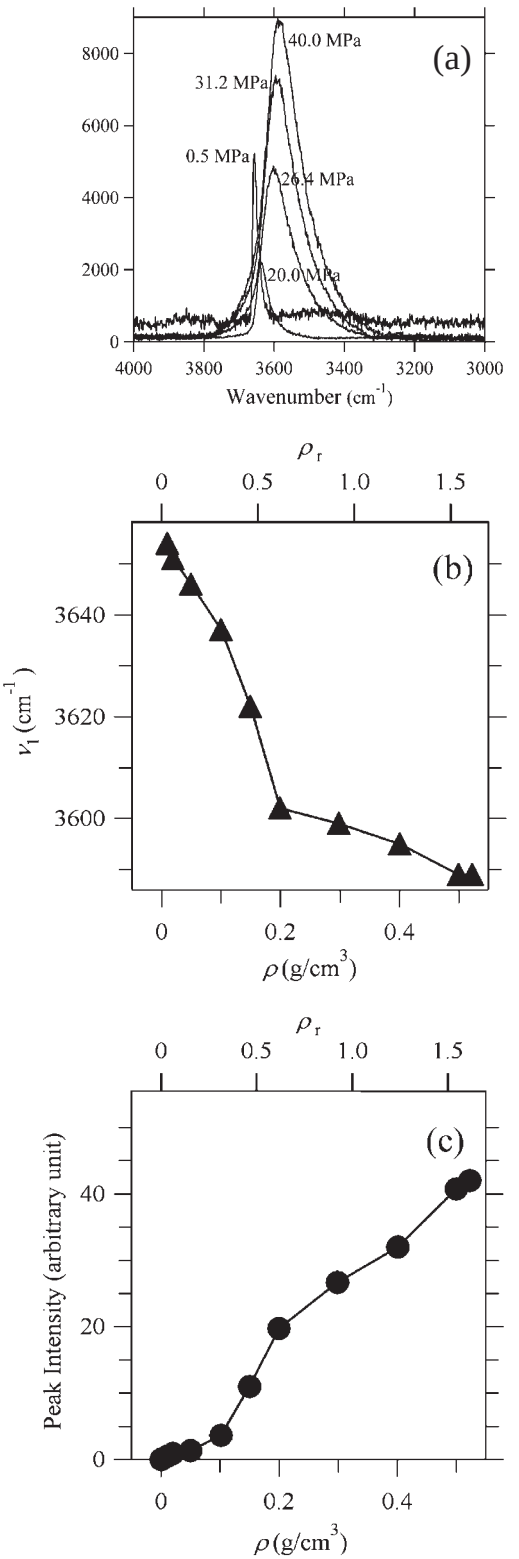

Fig. 4. (a) Raman spectral shift of water along the isothermal pressure change at 400 °C and 40.0, 31.2, 26.4, 20.0, and 0.5 MPa. Note that the peak intensity is arbitrary due to the difference in the measurement time. (b) Totally symmetric OH stretching peak (ν_1) position shift along the isothermal density change for water at 400 °C ($T_r = 1.04$). (c) Totally symmetric OH stretching peak intensity along the isothermal density change for water at 400 °C.

to the medium density region near ρ_c. We have succeeded in obtaining the clear OH stretching signals at densities as low as $\approx 3 \times 10^{-3}\,\mathrm{g\,cm^{-3}}$ (0.5 MPa at 400 °C; $T_r = 1.31$). The pressure dependence of the Raman spectrum of methanol at 400 °C is shown in Fig. 5a, and the peak position at each temperature examined is plotted against the reduced density ($\rho_r = \rho/\rho_c$, $\rho_c = 0.27\,\mathrm{g\,cm^{-3}}$) in Fig. 5b. Since the equation of state is not well established at temperatures above ≈350 °C,[4] the methanol density at 400 °C was determined from the ratio of the integrated intensity of the CH_3 peak to that of the diamond used as the cell window. The intensity ratio between the CH_3 and diamond peaks was obtained at lower temperatures, and it could be used to calibrate the methanol density. The integrated peak intensity for methanol is shown in Fig. 5c. In a manner similar to that for water, it increased nonlinearly with an increase in the density due to the intermolecular couplings.

At 250 °C that is close to T_c ($T_r = 1.02$), the profile of the density dependence of the methanol peak shift was similar to that of water at 400 °C ($T_r = 1.04$). Indeed, the slope of the density dependence changed around $\rho_r = 0.6$. At higher temperatures, in contrast, the characteristic change disappeared, and the peak position showed a fairly linear density dependence. To see the origin of such nonlinear density dependence, we compare our Raman results with the NMR ones. According to Ref. 43, the chemical shift of the OH proton of water represents the average number of hydrogen bonds derived from the O–H radial distribution function. Noticeably, the nonlinearity of the density dependence for water at 400 °C is relatively small in NMR chemical shift,[5] in contrast to the Raman measurements. This contrast is interpreted below in terms of the difference in the hydrogen-bonding effect detected in the spectroscopic measurements. For methanol hydrogen bonding, the nonlinearity in the NMR chemical shift is as evident as that observed in the Raman spectroscopy at 250 °C.[9,10] Such nonlinearity gradually disappears with an increase in the temperature for both the NMR chemical shift and Raman spectroscopic frequency shift. At 400 °C, the nonlinearity of the density dependence obtained by both NMR and Raman becomes barely observable. It should be noted that at 400 °C, the reduced temperature is much higher for methanol ($T_r = 1.31$; $T_c = 239$ °C) than for water ($T_r = 1.04$; $T_c = 374$ °C). Thus, the nonlinear dependence on the density appears only around T_c.

Mode-Specific Interpretation of the Density Dependence. As described above, the density dependencies of the Raman peak shift and the NMR chemical shift are parallel for methanol but not for water. This section presents a simple interpretation for this observation. The difference between water and methanol may be related to the direction of the response of OH stretching vibration to a given external field. Having only one OH, methanol can feel the effect of the external electric field directly in the direction of its OH. Thus, both Raman and NMR detect the effect of the field in the OH direction, and the results of the two measurements tend to be parallel to each other. For water, on the other hand, the totally symmetric Raman peak and the NMR chemical shift are related to different physical parameters: the former for the projection of the electric field onto the direction of the sum of two OH bond

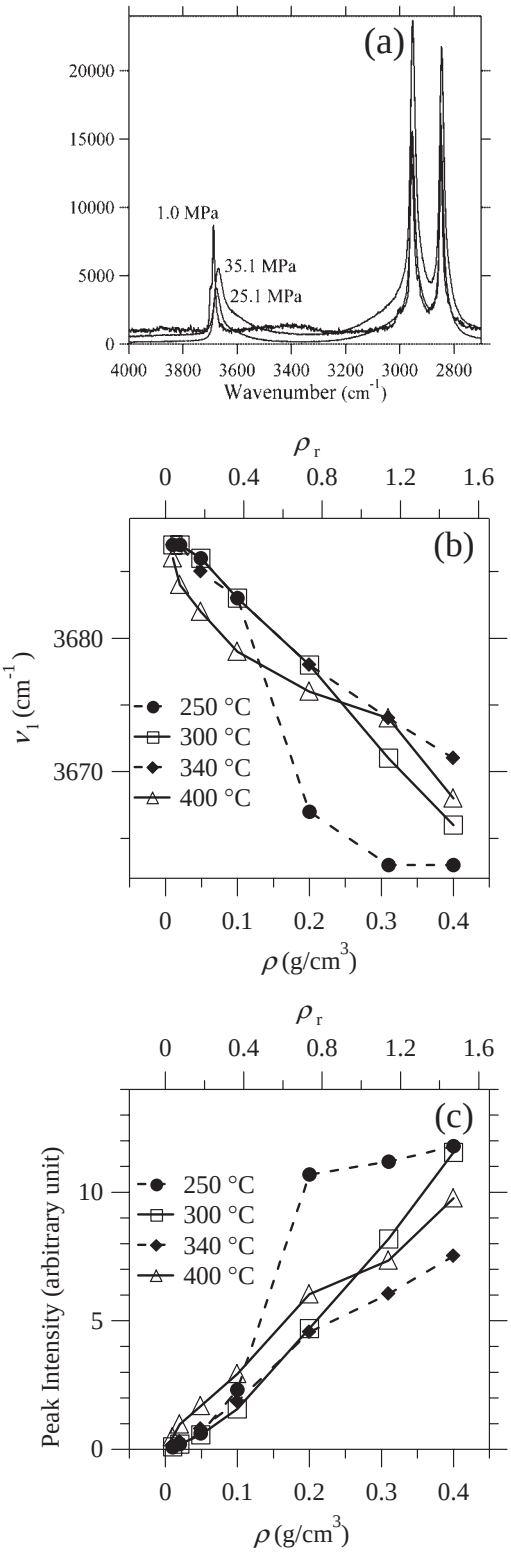

Fig. 5. (a) Raman spectral shift of methanol along the isothermal pressure change at 400 °C and 35.1, 25.1, and 1.0 MPa. Note that the peak intensity is arbitrary due to the difference in the measurement time. (b) OH stretching peak position (ν_1) along the isothermal density change at 250, 300, 340, and 400 °C ($T_r = 1.02$, 1.12, 1.20, and 1.31, respectively). (c) OH stretching peak intensity along the isothermal density change at 250, 300, 340, and 400 °C.

vectors, and the latter for the projection onto the direction of the OH bond itself. Thus, for water, an argument that takes into account the difference in the direction of the effect of electric field is necessary. A simplified "mode-specific" argument for water can be given as below.

Since the water molecule has three internal degrees of freedom (two OH stretchings and one HOH bending), its matrix of force constants is of 3×3 form.[42,43] When we focus only on the OH stretching motions,[44] the 2×2 submatrix of force constants can be written as

$$\begin{pmatrix} k_0 & -k' \\ -k' & k_0 \end{pmatrix} \tag{1}$$

with a coupling term k' for an isolated water molecule. The totally symmetric mode corresponds to the eigenvalue

$$\omega_0 = k_0 - k' \tag{2}$$

with a frequency lower than k_0. Note that k' is positive since the frequency is higher for the anti-symmetric mode than for the totally symmetric. When one of the OH groups is hydrogen-bonded, the matrix is modified as

$$\begin{pmatrix} k_0 - \Delta & -k' \\ -k' & k_0 \end{pmatrix} \tag{3}$$

and when both OH groups are hydrogen-bonded, the matrix is

$$\begin{pmatrix} k_0 - \Delta & -k' \\ -k' & k_0 - \Delta \end{pmatrix}. \tag{4}$$

Here, Δ denotes the effect of the hydrogen bonding. Since the hydrogen bonding is supposed to soften the OH bond, Δ is positive. The eigenvalues ω_1 and ω_2 corresponding to the totally symmetric mode (the lower frequency mode) for Eqs. 3 and 4 are then given, respectively, as

$$\omega_1 = k_0 - \Delta/2 - \sqrt{(k')^2 + \Delta^2/4}, \tag{5}$$

$$\omega_2 = k_0 - \Delta - k'. \tag{6}$$

The frequency reduction is larger in magnitude when the number of hydrogen-bonds changes from 0 to 1 than when it changes from 1 to 2. Indeed, the frequency reduces by

$$\omega_0 - \omega_1 = -k' + \Delta/2 + \sqrt{(k')^2 + \Delta^2/4} \tag{7}$$

with the change from 0 to 1, and by

$$\omega_1 - \omega_2 = k' + \Delta/2 - \sqrt{(k')^2 + \Delta^2/4} \tag{8}$$

with the change from 1 to 2. Evidently, the former is larger than the latter. Furthermore, since k' and Δ are positive, both of the frequency decrements are positive. Therefore, the build-up of the hydrogen bonds at a lower density has a stronger effect on the vibrational frequency for the totally symmetric OH stretching band.

In order to clarify how Raman spectroscopic observations are to be interpreted in terms of the dynamics and the local structure, further computational investigations that consider the coupling of the vibrational motions and molecular environments are inevitable. The connection to structural distribution or diversity will then be important as an approach complementary to NMR spectroscopy.

This work is supported by the Grant-in-Aid for Scientific Research (No. 15205004) from Japan Society for the Promotion of Science, by the Grant-in-Aid for Scientific Research on Priority Areas (No. 15076205) and the Grant-in-Aid for Creative Scientific Research (No. 13NP0201) from the Ministry of Education, Culture, Sports, Science and Technology, and from the CREST (Core Research for Evolutional Science and Technology) of Japan Science and Technology Corporation (JST).

References

1 R. W. Shaw, T. B. Brill, A. A. Clifford, C. A. Eckert, E. U. Franck, *Chem. Eng. News* **1991**, *69*, 26.

2 O. Kajimoto, *Chem. Rev.* **1999**, *99*, 355.

3 The International Association for the Properties of Water and Steam, IAPWS Formulation, **1995**.

4 K. M. Reuck, R. J. B. Craven, *Methanol* in *International Thermodynamic Tables of the Fluid State*, Blackwell Scientific, Oxford, **1993**, Vol. 12.

5 N. Matubayasi, C. Wakai, M. Nakahara, *J. Chem. Phys.* **1997**, *107*, 9133.

6 N. Matubayasi, N. Nakao, M. Nakahara, *J. Chem. Phys.* **2001**, *114*, 4107.

7 K. Yoshida, C. Wakai, N. Matubayasi, M. Nakahara, *J. Chem. Phys.* **2005**, *123*, 164506.

8 M. M. Hoffmann, M. S. Conradi, *J. Am. Chem. Soc.* **1997**, *119*, 3811.

9 M. M. Hoffmann, M. S. Conradi, *J. Phys. Chem. B* **1998**, *102*, 263.

10 N. Asahi, Y. Nakamura, *J. Chem. Phys.* **1998**, *109*, 9879.

11 S. Bai, C. R. Yonker, *J. Phys. Chem. A* **1998**, *102*, 8641.

12 W. Kohl, H. A. Lindner, E. U. Franck, *Ber. Bunsen-Ges. Phys. Chem.* **1991**, *95*, 1586.

13 J. D. Frantz, J. Dubessy, B. Mysen, *Chem. Geol.* **1993**, *106*, 9.

14 G. E. Walrafen, Y. C. Chu, G. J. Piermarini, *J. Phys. Chem.* **1996**, *100*, 10363.

15 G. E. Walrafen, W.-H. Yang, Y. C. Chu, *J. Phys. Chem. B* **1999**, *103*, 1332.

16 D. M. Carey, G. M. Korenowski, *J. Chem. Phys.* **1998**, *108*, 2669.

17 Y. Ikushima, K. Hatakeda, N. Saito, M. Arai, *J. Chem. Phys.* **1998**, *108*, 5855.

18 P. Postorino, R. H. Tromp, M.-A. Ricci, A. K. Soper, G. W. Neilson, *Nature* **1993**, *366*, 668.

19 R. H. Tromp, P. Postorino, G. W. Neilson, M. A. Ricci, A. K. Soper, *J. Chem. Phys.* **1994**, *101*, 6210.

20 K. Yamanaka, T. Yamaguchi, H. Wakita, *J. Chem. Phys.* **1994**, *101*, 9830.

21 A. K. Soper, F. Bruni, M. A. Ricci, *J. Chem. Phys.* **1997**, *106*, 247.

22 E. U. Franck, K. Roth, *Discuss. Faraday Soc.* **1967**, *43*, 108.

23 D. S. Bulgarevich, T. Sako, T. Sugeta, K. Otake, Y. Takebayashi, C. Kamizawa, M. Uesugi, M. Kato, *J. Chem. Phys.* **1999**, *111*, 4239.

24 D. S. Bulgarevich, K. Otake, T. Sako, T. Sugeta, Y. Takebayashi, C. Kamizawa, D. Shintani, A. Negishi, C. Tsurumi, *J. Chem. Phys.* **2002**, *116*, 1995.

25 T. Ebukuro, A. Takami, Y. Oshima, S. Koda, *J. Supercrit. Fluids* **1999**, *15*, 73.

26 T. Yamaguchi, *J. Mol. Liq.* **1998**, *78*, 43.
27 T. Yamaguchi, C. J. Benmore, A. K. Soper, *J. Chem. Phys.* **2000**, *112*, 8976.
28 T. Yamaguchi, N. Matubayasi, M. Nakahara, *J. Phys. Chem. A* **2004**, *108*, 1319.
29 a) R. Oparin, T. Tassaing, Y. Danten, M. Besnard, *J. Chem. Phys.* **2004**, *120*, 10691. b) J.-M. Andanson, J.-C. Soetens, T. Tassaing, M. Besnard, *J. Chem. Phys.* **2005**, *122*, 174512.
30 J. W. Tester, H. R. Holgate, F. J. Armellini, P. A. Webley, W. R. Killilea, G. T. Hong, H. E. Barner, *ACS Symp. Ser.* **1993**, *518*, 35.
31 P. E. Savage, *Chem. Rev.* **1999**, *99*, 603.
32 M. Watanabe, T. Sato, H. Inomata, R. L. Smith, K. Arai, A. Kruse, E. Dinjus, *Chem. Rev.* **2004**, *104*, 5803.
33 a) K. Yoshida, C. Wakai, N. Matubayasi, M. Nakahara, *J. Phys. Chem. A* **2004**, *108*, 7479. b) N. Matubayasi, M. Nakahara, *J. Chem. Phys.* **2005**, *122*, 074509.
34 a) Y. Nagai, S. Morooka, N. Matubayasi, M. Nakahara, *J. Phys. Chem. A* **2004**, *108*, 11635. b) Y. Nagai, N. Matubayasi, M. Nakahara, *J. Phys. Chem. A* **2005**, *109*, 3550. c) Y. Nagai, N. Matubayasi, M. Nakahara, *J. Phys. Chem. A* **2005**, *109*, 3558. d) S. Morooka, C. Wakai, N. Matubayasi, M. Nakahara, *J. Phys. Chem. A* **2005**, *109*, 6610. e) Y. Yasaka, K. Yoshida, C. Wakai, N. Matubayasi, M. Nakahara, *J. Phys. Chem. A* **2006**, *110*, 11082. f) S. Morooka, N. Matubayasi, M. Nakahara, *J. Phys. Chem. A* **2007**, *111*, 2697.
35 D. H. Rank, K. D. Larsen, E. R. Bordner, *J. Chem. Phys.* **1934**, *2*, 464.
36 D. Bender, *Phys. Rev.* **1935**, *47*, 252.
37 R. G. Inskeep, J. M. Kelliher, P. E. McMahon, B. G. Somers, *J. Chem. Phys.* **1958**, *28*, 1033.
38 K. Saitow, J. Sasaki, *J. Chem. Phys.* **2005**, *122*, 104502.
39 I. Skarmoutsos, J. Samios, *J. Chem. Phys.* **2007**, *126*, 044503.
40 N. Asahi, Y. Nakamura, *J. Chem. Phys.* **1998**, *109*, 9879.
41 T. Yamaguchi, N. Matubayasi, M. Nakahara, *Mol. Liq.* **2005**, *119*, 119.
42 E. B. Wilson, Jr., J. C. Decius, P. C. Cross, *Molecular Vibrations*, Dove Publication, New York, **1955**.
43 N. Matubayasi, C. Wakai, M. Nakahara, *J. Chem. Phys.* **1999**, *110*, 8000.
44 In the present simplified argument, the coupling with the bending mode is neglected since the frequency is separated from the two symmetric modes concerned.